

PACS numbers: 42.72.Bj; 52.80.–s
DOI: 10.1070/QE2012v042n02ABEH014266

Control of the UV flux of a XeCl dielectric barrier discharge excilamp through its current variation*

H. Piquet, S. Bhosle, R. Diez, M. Cousineau, M. Djibrillah, D. Le Thanh, A.N. Dagang, G. Zissis

Abstract. **The efficiency of the electrical power transfer to the gas mixture of a XeCl dielectric barrier discharge (DBD) exciplex lamp is analysed. An equivalent circuit model of the DBD is considered. It is shown that the excilamp power can be controlled by applying current to the lamp. This highly desired property is ensured by means of a specific power supply topology, whose concepts and design are discussed. The experimental prototype of a current-mode converter operating in the pulsed regime at pulse repetition rate of 50 kHz is presented and its capability to control the amount of energy transferred during each current pulse is demonstrated. The capability of this power supply to maintain specific operating conditions for the DBD lamp, with a very stable behaviour (even at a very low current, in the regime of a single discharge channel), is illustrated. The experimental results of a combined use of this converter and a XeCl excilamp are presented. The influence of the supply parameters on the 308-nm XeCl excilamp is analysed. The shape of the UV pulse of the lamp is experimentally shown to be similar to that of the current, which actually flows into the gas mixture. The UV radiation power is demonstrated to be tightly correlated to the current injected into the gas and controlled by the available degrees of freedom offered by the power supply. The measured UV output characteristics and performance of the system are discussed. Time resolved UV imaging of a XeCl DBD excilamp is used to analyse the mechanisms involved in the production of exciplexes at various power supply regimes. It is shown that a pulsed voltage source leads to formation of short high intensity UV peaks, while current pulses lead to formation of sustained discharge filaments. Based on the results of modelling of the above-mentioned operation conditions, the two power supply regimes are compared and analysed from the point of view of the UV power and radiative control.**

Keywords: *dielectric barrier discharge, exciplex, current regime, power supply, static converter, UV.*

* Reported at the IX International Conference on Atomic and Molecular Pulsed Lasers (Tomsk, 2009).

H. Piquet, M. Cousineau, M. Djibrillah, D. Le Thanh, A.N. Dagang, G. Zissis Université de Toulouse, LAPLACE, UMR CNRS INPT UPS, 2 rue Camichel, 31071 Toulouse Cedex, France;
email: Hubert.Piquet@laplace.univ-tlse.fr;
S. Bhosle OLISCIE, 175 chemin de la Pielle, 31600 Lherm, France;
R. Diez Electronics Department, Pontificia Universidad Javeriana, Bogotá, Colombia

Received 1 December 2009; revision received 4 October 2011
Kvantovaya Elektronika **42** (2) 157–164 (2012)
Submitted in English

1. Introduction

Dielectric barrier discharge (DBD) exciplex lamps are usually used with voltage-controlled electric generators: the classical solutions for laboratory experimental setups are built using large bandwidth linear amplifiers connected to step-up transformers [1, 2]. In industry oriented solutions, pulsed voltage sources are often employed, where switched voltages are generated by circuits with high-power semiconductors [3, 4]. When applying such voltages, the DBD lamp induces a very narrow current spike in the circuit. Analysis of the UV radiation response of the excilamp shows a similar time dependence for the UV radiation power. The UV spikes have also a very short duration, compared to the operating period of the whole system. The characteristics of the current spikes (magnitude, duration, frequency) are really difficult to control with the help of voltage-controlled electric generators [5, 6].

The aim of this paper is to consider the power supply as a means to control UV emission of the excilamp. Based on the analysis of the cause and effect of the power transfer between the power supply and the lamp, we have favoured current-controlled topologies. A specific solution is described, and key aspects of the design of the current-controlled power supply, being absolutely different from the classical voltage-controlled source, are considered. We also present the working characteristics of this electric generator connected to the XeCl excilamp. They confirm the validity of our hypothesis on the necessity of using current-controlled power supplies.

2. Mechanisms for current-controled UV emission

From a modelling point of view, we have demonstrated [7] the correspondence between the input current and the UV flux of an excilamp. In this section, using a partial differential equation (PDE) model, we analyse the mechanisms involved.

2.1. PDE model of an excilamp

We have developed a PDE-based model, considered in detail in [8], for a planar double-dielectric layer xenon excilamp. The plasma is assumed homogeneous and side effects around the electrodes are neglected. Therefore, computations performed are one-dimensional (along the axis of the system geometry) and similar to those presented in [9]. The thickness of the dielectric layers is 2 mm, the gas gap is 4 mm and the xenon filling pressure is 5.33×10^4 Pa (400 Torr). The model solves the drift-diffusion equations for particles by using Poisson's equation.

A voltage supplied DBD is modelled by applying a potential on both outer sides of the dielectrics. This leads to two

Dirichlet boundary conditions for Poisson's equation. Usually, one side is grounded and the other is set to the voltage chosen for the modelling. A current supplied DBD is modelled by grounding one side of the outer surface of a dielectric and by applying an electric field, which is proportional to the time integral of the current, on the outer surface of the other dielectric:

$$\boldsymbol{E}(x_0, t) = \frac{1}{\varepsilon}\int_0^t \boldsymbol{j}(x_0, t)\,\mathrm{d}t, \tag{1}$$

where $\boldsymbol{E}(x_0, t)$ is the electric field at the outer surface of the dielectric; ε is the permittivity of the dielectric; $\boldsymbol{j}(x_0, t)$ is the current density flowing through the dielectric. Equation (1) corresponds to a Neumann boundary condition for Poisson's equation. The model relies on the local field approximation and, consequently, the transport coefficients and source parameters depend on the electric field. These coefficients and source parameters are calculated by Bolsig [10]. Once solved, the model can display the spatiotemporal evolution of the plasma density and the electric field.

2.2. Excimer production for various waveforms

The mechanism which has the major impact on the development of the discharge is the propagation of the ionisation front toward the dielectric acting as a cathode. This ionisation front markedly affects the current waveform and leads to a massive production of charges, excited particles and especially excimers [11]. As a result, the UV flux (emitted by excimers) of an excilamp is directly related to the development of the ionisation front. The microscopic interactions between this front motion, the electric field in the cathode sheath and the current density can be analysed by using the model described above.

Consider first a steady-state DBD produced by a high-voltage pulse. The electronic cloud drifts in the applied field, leaving behind a positively charged area: the cathode sheath. A strong electric field develops here, leading to acceleration of electrons emitted from the dielectric wall in cathode phase. These electrons produce an avalanche, involving the development of an ionisation front and the deposition of charges on the dielectrics which compensate for the applied electric field. Consequently, the discharge mechanism stops. The resulting time evolution of the current and optical output is characterised by a strong peak, corresponding to the ionisation front motion. The scheme of the described mechanism is presented in Fig. 1a.

When the characteristic time of changes in the applied voltage exceeds the characteristic time of ionisation front evolution, the mechanism is the same as that describes above. Hence, the current and optical peaks occur for an applied voltage threshold. The results of PDE modelling for a 8-kV sine-wave applied voltage at 50 kHz are presented in Fig. 1b.

We can say from the previous reasoning that the time evolution of the ionisation front, corresponding to the time evolution of the UV flux, is purely defined by the plasma kinetics and the voltage step value. A change in the ionisation front evolution characteristic time can be achieved if the electric field in the cathode sheath changes in a shorter time. This can be done externally by varying the applied voltage. In this case, the UV flux would globally behave as an image of the applied voltage time derivative. As a result, an optical control of the lamp could be achieved through control of the slope (or derivative) of the applied voltage.

When a current-controlled power supply is used, the injected current flows in the centre of a steady-state DBD as conduction current. At an early stage, this current corresponds to the flux of the electronic cloud. However, an electric field increases behind the electronic cloud, in the cathode sheath. The ionisation front develops and leads to a strong excimer production and, consequently, to a UV flux peak. After this stage, stable current maintains the ionisation area near the cathode dielectric, which feeds the plasma bulk with charges, so as their flux matches the applied current. Therefore, this last stage corresponds to an uninterrupted excimer production. Figure 2 presents the UV flux of the modelled excilamp, maintained by various current waveforms.

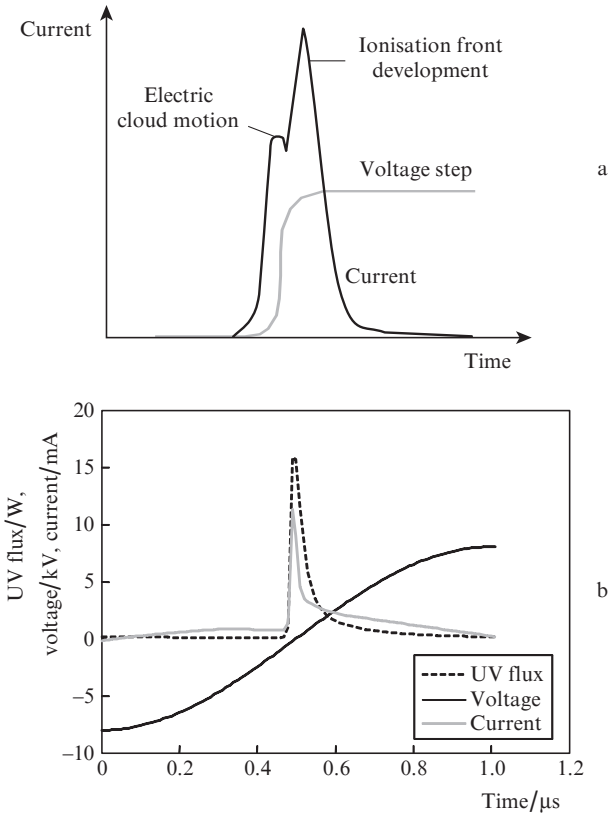

Figure 1. Shape of the current for a voltage supplied DBD in the case of a step voltage pulse (a) and the results of modelling for a 50-kHz, 8-kV maximum amplitude voltage.

It follows from the discharge mechanisms described above that the UV radiation of an excilamp can be controlled either by controlling the applied voltage time derivative or by applying the current. Actually, these two situations are quite similar, taking into account the capacitive nature of a DBD. However, from the point of view of power electronics, it is easier to design a current source circuit than a voltage derivative controlled source. Such a current source design is discussed below.

3. Power transfer

In this section, we analyse the power transfer between an electric generator and a DBD excilamp. An equivalent circuit for a DBD device [1, 12], which has proven it suitability in the case of excimer lamps, is presented in Fig. 3.

As capacitors use is made of the capacitance of the dielectric walls (C_{diel}) and the capacitance of the gas (C_{gas}). This gas capacitor is the main electric characteristic of the gas, as long as the discharge is switched off (OFF state). The conductance of the gas G_{gas} describes the behaviour of the gas when the

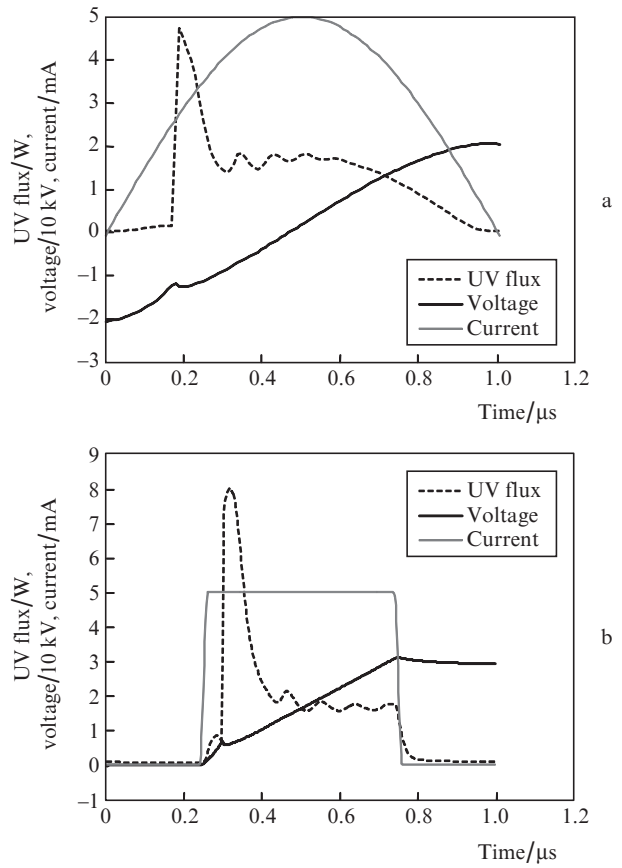

Figure 2. UV flux of the modelled excilamp maintained by various current waveforms.

discharge is switched on (ON state). The voltage across the gas u_{gas} is the state that defines the state (ON, OFF) of the system. The conductance of the gas is the adequate choice to evaluate the current flowing in the gas, i_{gas}. The behaviour of G_{gas} is described by the equation

$$\frac{dG_{gas}}{dt} = K_{gen}\left[1 + \exp\left(\frac{U_{th} - |u_{gas}|}{\Delta U}\right)\right]^{-1} - K_{ext}G_{gas} + K_{pro}|i_{gas}|. \quad (2)$$

The three terms of the right-hand side describe respectively three phenomena: breakdown, which occurs when u_{gas} reaches the threshold voltage U_{th}; the extinction of the generated particles (K_{ext} controls the extinction rate); the generation of the excited particles, which is assumed to be proportional to the magnitude of the current flowing in the gas, i_{gas}.

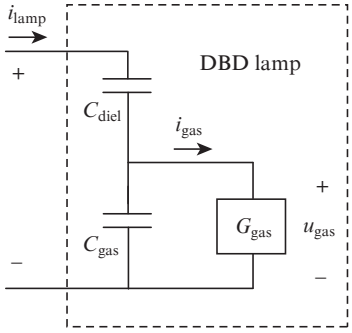

Figure 3. Equivalent circuit of the excilamp model.

The identification of the parameters of the model is achieved by means of an automated method: the set of values [K_{gen}, U_{th}, ΔU, K_{ext}, K_{pro} introduced in equation (2)] is iteratively adjusted to obtain a good agreement between experimental and simulated waveforms. This approach and its implementation are presented in detail in [13]. The parameters of the 60-W XeCl excilamp used in experiments are given in Table 1. The behaviour of the circuit (Fig. 3) is described by the electric differential equations:

$$u_{gas} = u_{lamp} - \frac{1}{C_{diel}}\int i_{lamp}\,dt, \quad (3)$$

$$i_{gas} = G_{gas}u_{gas}. \quad (4)$$

Table 1. Parameters of a 60-W Xe/Cl excilamp.

Parameter	Values	
	Initial	Final
U_{th}/V	1500	1800
ΔU/V	20	2.9
K_{gen}/Ω s^{-1}	130	2×10^4
K_{ext}/s^{-1}	2.7×10^6	1×10^6
K_{pro}/V^{-1} s^{-1}	1835	100
C_{diel}/pF	39.81	40.03
C_{gas}/pF	13.07	13.87

Once the parameters of the model are determined, the waveforms of G_{gas}, u_{gas} and i_{gas}, which are nonmeasurable quantities, are calculated. The input data of this process are the measured waveforms of u_{lamp} and i_{lamp}, and equations (2), together with (3) and (4), are used in calculations. Note that the formulation of these state equations favours the expression of the actual causality chain between the physical quantities: derivatives are avoided and the current i_{lamp} in the lamp determines the behaviour of the whole system.

The voltage–current (i_{gas}–u_{gas}) characteristic of the lamp used in the experiments is presented in Fig. 4. The data used to define the parameters have been obtained in the experiments with a classical sinusoidal high voltage supply.

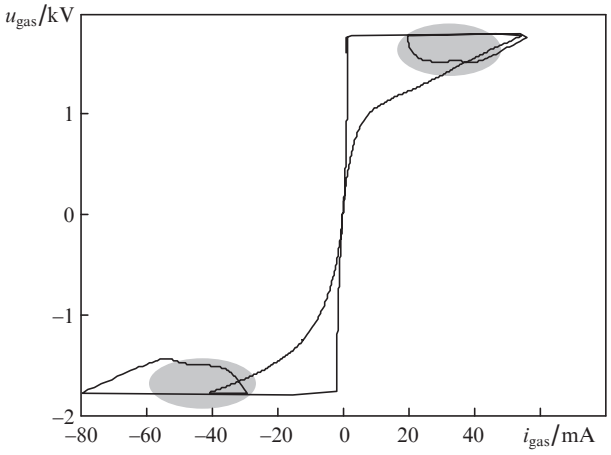

Figure 4. Voltage–current (i_{gas}–u_{gas}) characteristic of the gas. Grey areas show the desired operation regions.

This hysteretic form is characterised by a voltage plateau, with a value near the threshold voltage, U_{th}. When the gas is in the ON state, the operating point remains on this plateau: the gas voltage u_{gas} remains constant in a quite large domain of the current values, i_{gas}. Thus, the instantaneous power transferred from the supply to the gas, being the $i_{gas}u_{gas}$ product, is directly controlled by the i_{gas} current. In Fig. 4, the areas where this assumption appears to be valid are grey. Below, we describe the ways of controlling the operating point of the discharge which should remain in these areas. Despite the fact that the power supply cannot directly control the i_{gas} current (see Fig. 3), the generator can control the i_{lamp} current, which will be shown later to be very similar to i_{gas}, except when the discharge is OFF.

4. Current-controlled supply for excilamps

According to the conclusions of the previous section, the mostly desirable characteristic of a power supply for a DBD excilamp is the ability of controlling the current circulating in the lamp. Additionally, the electric generator must supply a current, whose mean value is zero, at a timescale corresponding to the operating period, because of the capacitive characteristic of the lamp. To this end, several topologies have been considered [14]. The circuit in Fig. 5 presents one of them, with a circuit which inverts the sign of the current in the lamp after each half period by the switches S1 and S1′ [both are connected with one of the primary windings of the transformer (oppositely pointed)] as well as controls the amount of energy supplied to the lamp during each half operating period by the switch S0.

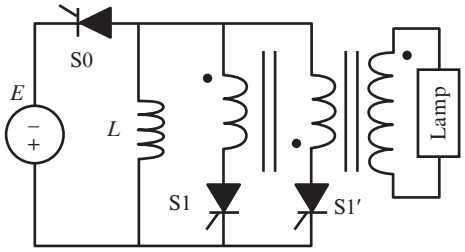

Figure 5. Current-controlled power supply.

4.1. Operation regime

Figure 6 presents expected ideal waveforms (inductance current L is shown by the grey line and current in the lamp – by the black line), and the operating cycles, according to the states of the switches of the converter. These curves are obtained with a circuit simulation program [15, 16]: the step-up transformer is supposed ideal (the step-up ratio of the transformer n) and the lamp is sketched, according to the characteristic of Fig. 4, as a $\pm U_{th}$ voltage source connected in series with the dielectric capacitor C_{diel}.

A very important feature of this converter is seen from Fig. 6: the duration of the cycles A and C, when the energy is stored in the L inductance ($\frac{1}{2}LI_{L0}^2$), controls the amount of energy injected into the lamp during each half period. The stored energy is transferred through the transformer into the lamp during the oscillating cycles B and D, involving L and C_{diel}.

The duration of the cycles B and D, $t_{discharge}$, is defined by the values of C_{diel}, L, n and I_{L0} [14]. They naturally terminate

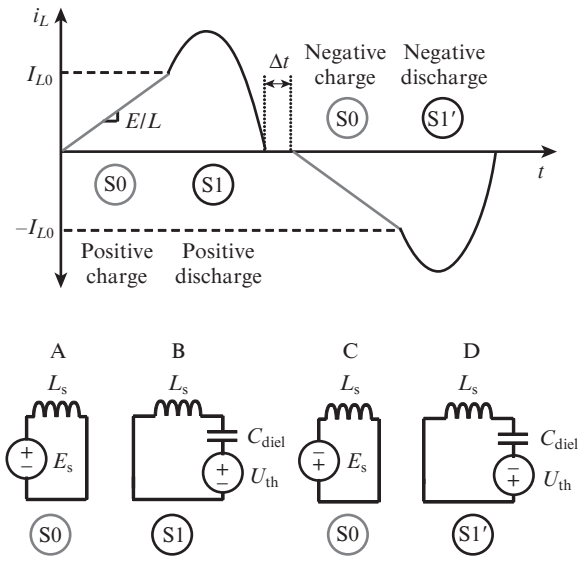

Figure 6. Operating cycles.

when the i_L current becomes zero (spontaneous turn-off of the thyristor-like switches). A blanking time interval, Δt, added between the cycles B and C and between D and A, is introduced to adjust the relaxation time interval between two current pulses in the lamp.

These discharge and blanking times define, with t_{charge} that is the duration of the cycles A and C, the operating period of the converter:

$$T = 2(t_{charge} + t_{discharge} + t_{blanking}) = 1/f_{switch}. \quad (5)$$

The I_{L0} value of the current in the inductance L at the end of the cycles A and C, defined by the controlled switching-on of either S1 or S1′ to start the B or D cycles, is a direct method for controlling the power transferred to the lamp

$$I_{L0} = Et_{charge}/L, \quad (6)$$

$$P_{lamp} = 2f_{switch}(\tfrac{1}{2}LI_{L0}^2). \quad (7)$$

where f_{switch} is the operating frequency of the supply.

4.2. Design and control considerations

In designing such a supply, it is required that the three switches of the converter have the thyristor-like operating characteristics (unidirectional current in the ON state, bidirectional voltage in the OFF state with controlled switching-on and spontaneous switching-off). The usual operating frequencies of classical devices are not compatible with the frequency expected in the considered application (several kHz). Therefore, a synthesised circuit based on a power MOSFET connected in series with a high voltage fast diode and an electronic control circuit has been especially studied and designed.

A critical point in constructing the current-controlled supply is the design of the step-up transformer. It requires a very specific construction: indeed, the parasitic parameters of the windings (especially the high voltage winding) have a critical effect on the quality of the waveforms and of the operating conditions. The magnetising inductance must have a large enough value to avoid current flow in the lamp during the

cycles A and C. Leakage inductances should be minimised to avoid high frequency oscillations during the cycles B and D. The capacitance of the secondary winding should be minimised as well: it can divert a significant percentage of the current injected into the lamp.

One can see from equations (5)–(7) that the proposed power supply offers several degrees of freedom (DOF) to achieve the control of the power transfer:

(i) t_{charge} is used to set the values of the current (I_{L0}/n) injected in the lamp; it also defines the energy transferred into the lamp during the next pulse.

(ii) $t_{\text{discharge}}$ is not directly controlled and depends on the value of I_{L0}.

(iii) t_{blanking} is adjustable and defines the duration of the relaxation time interval (no current injected into the lamp) and contributes to the definition of the operating frequency.

In the experimental setup, these DOF are managed by a DSP-FPGA-based control unit, which accurately defines all the events through the firing orders of each power switch and offers possible transient analysis and time domain measurements.

5. Characteristics of generation of UV radiation

5.1. Electric parameters of the supply

A prototype of the proposed supply has been implemented (the main characteristics are summarised below) and connected to an excilamp.

Switching frequency f_{switch}/kHz	50
Primary inductance L/μH	160
Step-up transformer ratio n	12
Voltage supply E/V	150
Current at the end of the cycle A or C I_{L0}/A	$\leqslant$ 1.5
Measured electric efficiency η (%)	70

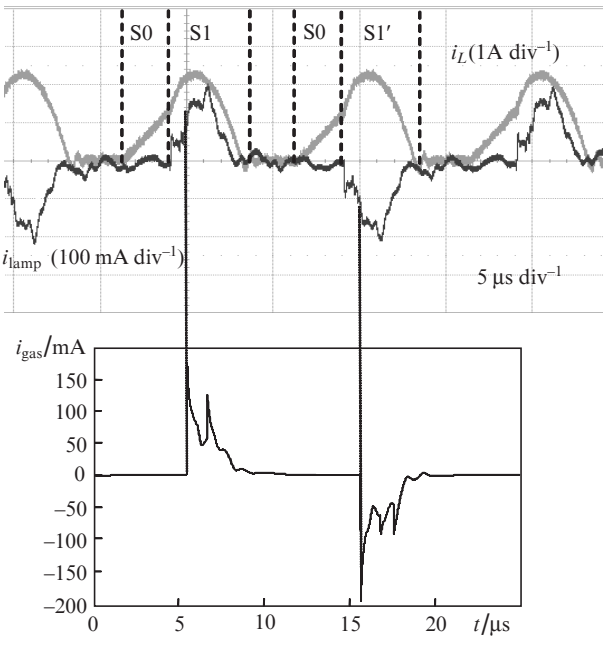

Figure 7. Main characteristics of the supply; measured currents i_L (grey) and i_{lamp} (black, top) and the calculated current i_{gas} (bottom).

The excilamp consists of two 130-mm-long coaxial quartz tubes, 43 mm and 23 mm in outer diameter, which are the two dielectric barrier layers between outer and inner electrodes. The inner electrode is an aluminium rod connected to a pulsed current source and the outer is a grounded wire mesh. The excilamp is sealed with a mixture of chlorine (lower than 0.5%) and Xe at a total pressure around 150 mbar.

Figure 7 shows the measured currents in the inductance L (i_L) and in the lamp (i_{lamp}), which are in good agreement with theoretical results. Higher frequency oscillations appearing in the i_{lamp} signal are caused by the mentioned parasitic elements of the step-up transformer. Using the model described in section 2, we can calculate nonmeasurable quantities and the current flowing through the gas, i_{gas}.

5.2. UV emission

We have also developed an optical system connected to the power supply. It offers time-resolved (with synchronisation of the control signals of the power supply) and mean measurements of the produced light, both in the visible and UV domains (see section 6). The comparison between the shapes of the instantaneous UV power level and the calculated cur-

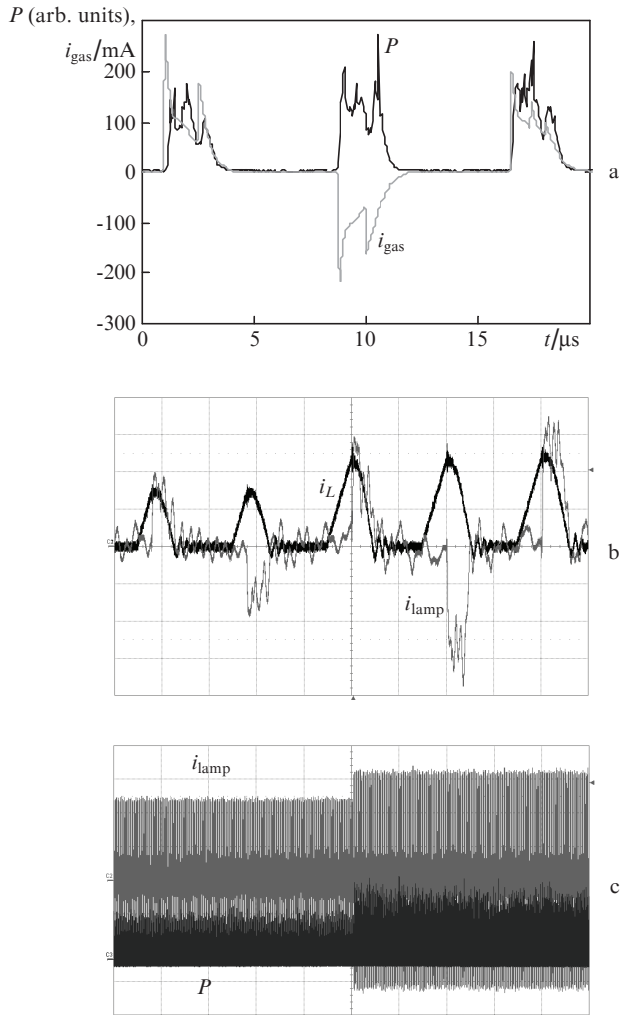

Figure 8. (a) Shapes of the measured instantaneous UV power compared to the calculated current i_{gas}, (b) instantaneous control of the current i_{lamp}, and (c) UV lasing controlled by the power supply.

rent i_{gas} is given in Fig. 8a. Though using a sine voltage supply, results presented in [17] are in very good agreement, concerning the tight correlation between the two waveforms.

Synchronisation between the power supply and the optical measurements makes it possible to establish the similarity of the waveforms. Several similar measurements, with different pulse durations i_{gas}, have been performed and give identical conclusions: UV emission is very tightly correlated to the current i_{gas} in the gas, and any changes in the latter (by means of one of the DOF of the supply) is immediately followed by the same change in the UV flux. The time scales concerning the use of this property for UV emission control start from half the operating period of the converter.

Figure 8b shows the capability of the supply to change the current in the lamp at the half-period time scale. Figure 8c demonstrates the capability of the supply to set the UV level by means of the controllable current i_{lamp}, even in transient conditions.

The quality of the generated UV has been studied at different levels of power injection (controlled by the duration t_{charge}): Fig. 9a proves that the spectral quality of the radiation of the lamp is not affected by the transferred power.

Taking into account the mean UV power (measured with a 308-nm radiometer), the DOFs of the supply are used to study the correlation between the relative UV power and the injected power for several operating frequencies.

It follows from Fig. 9b that the UV power increases with the charge duration t_{charge}, which defines the energy transferred to the lamp [theoretically, according to equations (6) and (7), with a quadratic shape], and with the switching frequency, which is proportional to the injected electric power [see equation (7)]. One can see from Fig. 9b that the curve corresponding to 50 kHz is very close to the curve corresponding to 55 kHz. This can be interpreted as a better electrical-to-optical power conversion of the lamp at 50 kHz. The last result is very interesting, making it possible to suggest that the current-mode power supply can be used to determine the optimal operating frequency of the lamp.

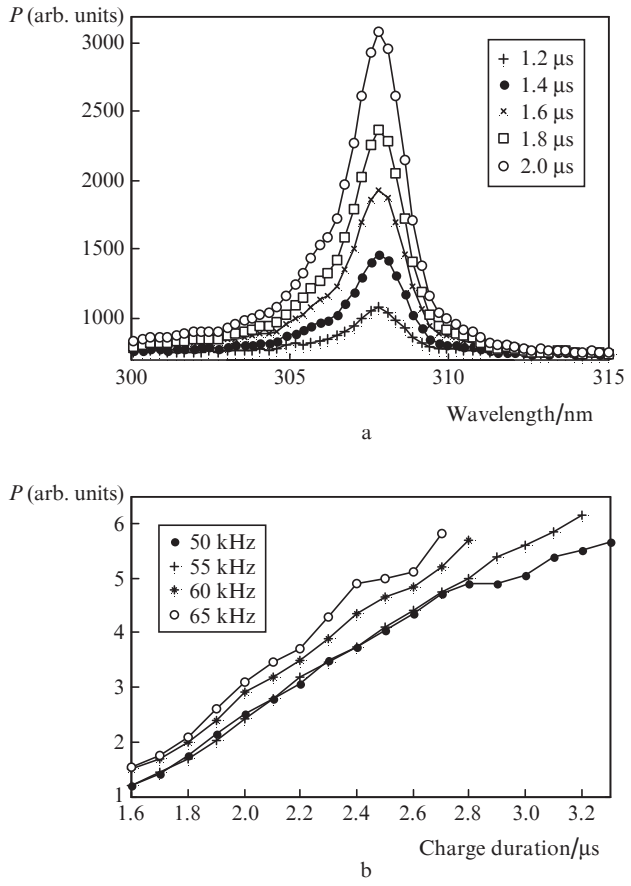

Figure 9. (a) Power distribution of the generated UV at different power injection levels, (b) dependence of the relative UV power on the charge time t_{charge} for several operating frequencies.

6. UV imaging of the excilamp

Figure 10 presents a scheme of high speed UV imaging of the excilamp supplied by a voltage and current pulsed power supply. A quartz lens through a UV filter focuses the UV part of the excilamp image on the photocathode of an intensified CCD camera (Roper Scientific PI-MAX). The controller of the camera controls synchronisation of acquisitions with the electrical gating signals of the excilamp power supply. The oscilloscope registers these electrical measurements during the acquisition. The images coming from the camera, synchronised with the electrical waveforms, are transferred to the computer.

The excilamp is fed by a 60-kHz pulsed current or voltage power supply. The electrical waveforms and corresponding

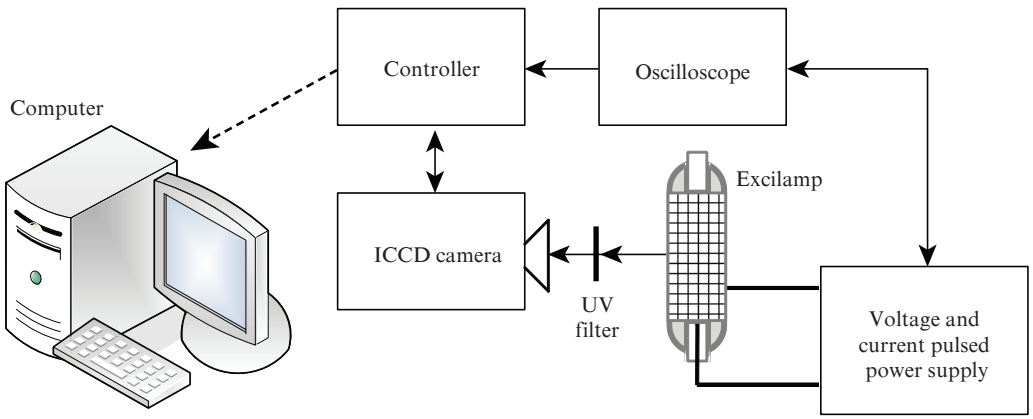

Figure 10. Scheme of the high speed UV imaging experimental system.

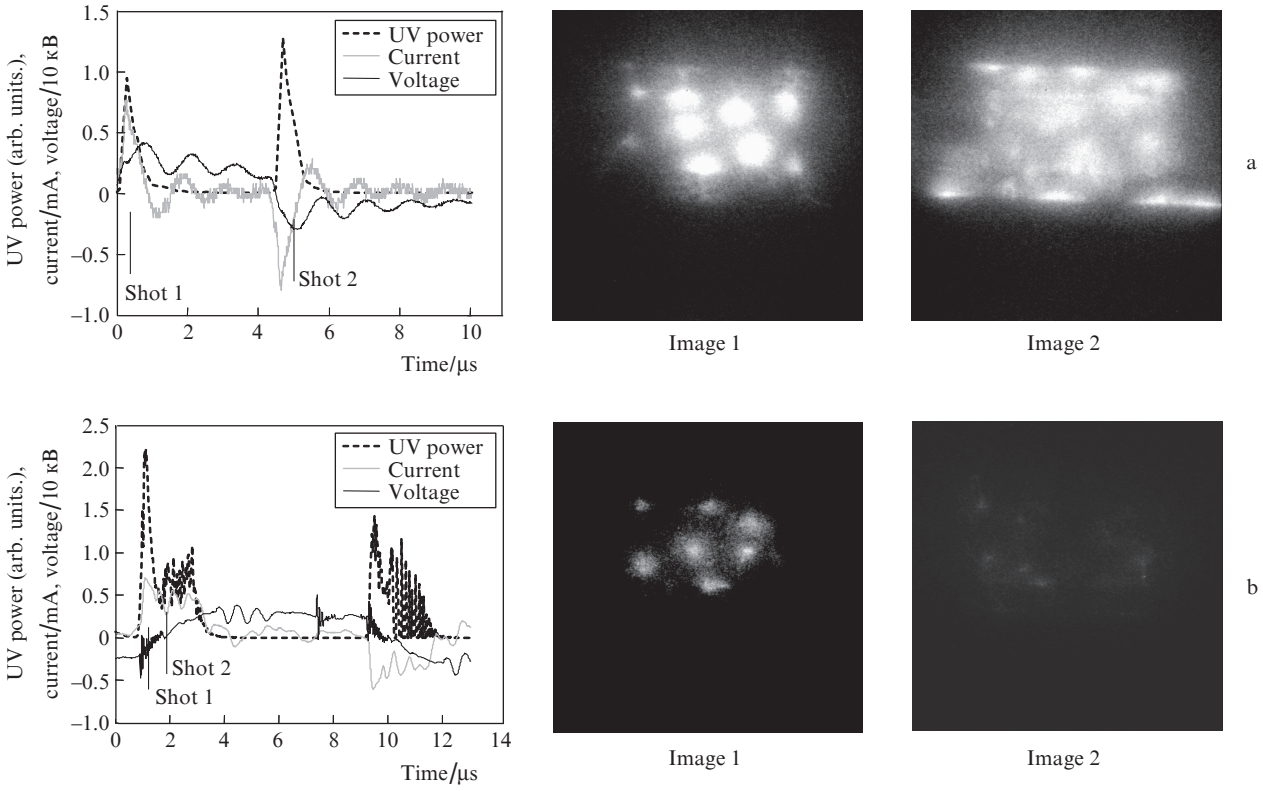

Figure 11. UV imaging of the excilamp in the case of (a) a pulsed voltage source and (b) a pulsed current source.

UV images are presented in Fig. 11. One can see that in the case of a voltage source, two strong UV peaks appear, corresponding to the current peaks [images 1 and 2, panel (a)]. Between two voltage rising or falling fronts, UV emission is not observed. For a current supplied excilamp, the current peak induced by the power supply lasts approximately 3 μs and UV emission is still visible during this time. One can see from images 1 and 2 in panel (b) that a filamentary discharge structure is sustained and lasts as long as the current is maintained. This demonstrates that the current control of a DBD leads to a control of the discharge mechanisms and that ionisation fronts are sustained in filamentary channels as long as the current is maintained.

7. Conclusions

The concept of a current-controlled static converter has been presented to control the power transfer to the DBD lamp. The proposed technique has shown its capability to control the current and the power injected in the lamp at each half operating period.

A device for UV optical measurements, synchronised with the power supply, has been connected to the experimental setup. Its use confirmed the fact that UV emission is directly controlled by the current flowing into the gas, which in turn can be controlled by the current injected in the lamp.

The proposed static converter offers two main degrees of freedom to define the operating conditions of the system: the injected power level at each half period and the frequency. These DOFs have been studied and UV emission has been shown to be tightly correlated to the electric power. Specific behaviour (depending on the operating frequency) has been observed, which suggests that the power supply presented in this paper can be useful for further studies, carried by plasma physicist, in order to define the optimal operating parameters of a DBD lamp.

Acknowledgements. The authors thank Dermoptics (Quantel Group) for their support in providing their patented lamp for the experimental part of the work. Part of this work is a French-Colombian cooperation, supported by the ECOS-Nord/COLCENCIAS/ICETEX program.

References

1. Kogelschatz U. *Plasma Chem. Plasma Process.*, **23**, 1 (2003).
2. Bhosle S., Zissis G., Damelincourt J.J., Capdevila A., Gupta K., Dawson F.P., Tarasenko V.F. *Proc. IEEE IAS Conf.*, **4**, 1784 (2006).
3. Sosnin E.A., Erofeev M.V., Tarasenko V.F., Shitz D.V. *Instrum. Exp. Techniques*, **45** (6), 838 (2002).
4. Lomaev M.I., Sosnin E.A., Tarasenko V.F., Shits D.V., Skakun V.S., Erofeev M.V., Lisenko A.A. *Instrum. Exp. Techniques*, **49** (5), 595 (2006).
5. Oda A., Sugawara H., Sakai Y., Akashi H. *J. Phys. D: Appl. Phys.*, **33** (12), 1507 (2000).
6. Mildren R.P., Carman R.J. *J. Phys. D: Appl. Phys.*, **34** (1), L1–L6 (2001).
7. Bhosle S., Piquet H., Diez R., Tarasenko V.F., Erofeev M.V., Zissis G. *Proc. 11th Int. Symp. High Pressure, Low Temperature Plasma Chemistry (HAKONE XI)* (Oleron Island, France, 2008).
8. Bhosle S., Zissis G., Damelincourt J.J., Capdevila A. *Proc. XVI Int. Conf. Gas Discharge and Appl. (GD-2006)* (Xi'an, China, 2006).
9. Oda A., Sakai Y., Akashi H., Sugawara H. *J. Phys. D: Appl. Phys.*, **32**, 2726 (1999).
10. *The Siglo Database* (CPAT & Kinema Software, 1995).

11. Piquet H., Bhosle S., Diez R., Toumi A., Zissis G. *Proc. SPIE Int. Soc. Opt. Eng*., **6938**, 693810 (2008).
12. Vongphouthone S., Piquet H., Foch H. *Eur. Phys. J. Appl. Phys*., **15**, 123 (2001).
13. Diez R., Salanne J.P., Piquet H., Bhosle S., Zissis G. *Eur. Phys. J. Appl. Phys*., **37**, 307 (2007).
14. Diez R., Piquet H., Bhosle S., Blaquière J.M., Roux N. *IEEE Int. Symposium on Indus. Electronics*, **1**, 62 (2008).
15. http://www.powersimtech.com.
16. http://www.synopsys.com.
17. Borisov V.M. et al. *Kvantovaya Elektron.*, **25** (4), 308 (1998) [*Quantum Electron*., **28** (4), 297 (1998)].